



25 W 2 μm broadband polarization-maintaining hybrid Ho- and Tm-doped fiber amplifier

ROBERT E. TENCH,^{1,*}  CLEMENT ROMANO,^{1,2,3}  AND J.-M. DELAUAUX¹

¹Cybel LLC, 1195 Pennsylvania Avenue, Bethlehem, Pennsylvania 18018, USA

²Institut Telecom/Telecom ParisTech, 46 Rue Barrault, 75634 Paris, France

³Fraunhofer IOSB, Gutleuthausstraße 1, 76275 Ettlingen, Germany

*Corresponding author: robert.tench@cybel-llc.com

Received 21 February 2019; revised 22 April 2019; accepted 25 April 2019; posted 26 April 2019 (Doc. ID 360684); published 20 May 2019

We report the design, evaluation, and performance of a polarization-maintaining (PM) fiber amplifier with a CW output power of >25 W at 2051 nm and a high input signal dynamic range of 34 dB at 25 W. To improve both the output power and dynamic range performance of previous amplifiers, we propose a PM hybrid design with a single-clad Ho-doped preamplifier (HDFA) followed by a double-clad Tm-doped power amplifier (TDFA). The role of the Ho-doped fiber preamplifier is to provide large input signal dynamic range, low noise figure, and moderate output power over an operating bandwidth from ≈ 2 – 2.1 μm . The role of the Tm-doped fiber power amplifier is to offer power amplification with good efficiency, taking full advantage of 2-for-1 ion-ion interactions, with the possibility of scaling up the output power to values much higher than 25 W. Our hybrid Ho-Tm-doped design provides a PM fiber amplifier with a combination of large input signal dynamic range, low noise figure, broad operating bandwidth, and high output power. Simulations of the hybrid HDFA/TDFA performance agree relatively well with experimental data. © 2019 Optical Society of America

<https://doi.org/10.1364/AO.58.004170>

1. INTRODUCTION

Current developments in lidar [1] and atmospheric sensing experiments [2,3] highlight the need for multiwatt, large bandwidth, high dynamic range polarization-maintaining (PM) optical amplifiers in the eye-safe 1.9–2.15 μm band. So far, as an illustration of the previous state of the art for high-power devices, multiwatt Tm-doped fiber amplifiers (TDFAs) have been demonstrated by Goodno *et al.* [4] with an output power of 608 W at a signal wavelength of 2040 nm. As for Ho-doped fiber amplifiers (HDFAs) Hemming *et al.* [5] have reported output powers of 265 W at 2110 nm. For this HDFA, a double-clad Ho-doped fiber pumped by high-power fiber lasers made the configuration complex and yielded an optical slope efficiency of 41%. Both of these achievements were with standard (non-PM) fiber.

Recently, we demonstrated a hybrid single-clad/double-clad TDFA with 20 W output and a dynamic range of >12 dB in the 2 μm band [6]. We have also reported single-clad PM HDFAs with output powers of up to 6.7 W CW at 2051 nm [7–9], gains as high as 60 dB, and a dynamic range of 40 dB. The scaling of output power in this amplifier is limited by the amount of pump power that can be coupled into the single-clad single-mode active fiber, and by the eventual onset of nonlinearities such as stimulated Brillouin scattering (SBS).

To scale up both output power and dynamic range performance, we propose here a new PM hybrid HDFA/TDFA with a single-clad Ho-doped preamplifier followed by a double-clad Tm-doped power amplifier. The role of the Ho-doped fiber preamplifier is to provide large input signal dynamic range, low noise figure (NF), and reasonable P_{out} over an operating bandwidth from ≈ 2 – 2.15 μm . The role of the Tm-doped fiber power amplifier is to offer power amplification with good efficiency, taking full advantage of 2-for-1 ion-ion interactions from 793 nm pumping, with the possibility of scaling up the output power to values much higher than 25 W. Our new hybrid Ho-Tm-doped amplifier design therefore provides a combination of large dynamic range, low NF, broad operating bandwidth, and high output power.

In this paper, we present the evaluation and performance of a PM hybrid HDFA/TDFA with output power of $P_{\text{out}} \geq 25$ W at 2051 nm and a high dynamic range of 34 dB [10]. Our paper is organized as follows: first, we present the experimental setup and optical architecture of the three-stage PM hybrid HDFA/TDFA. Next, we give data for the single-clad Ho-doped fiber and the double-clad Tm-doped fiber and discuss our methods for simulating fiber amplifier performance. Then we describe the experimental performance of the amplifier with a single-frequency input signal at $\lambda_s = 2051$ nm. We compare our experimental results with a

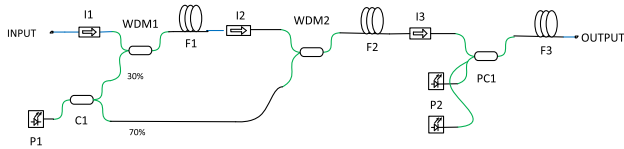


Fig. 1. Optical design of three-stage hybrid PM HDFA/TDFA.

steady-state simulation of amplifier performance and demonstrate good agreement between theory and data. Finally, we discuss amplifier and performance optimization for the three-stage amplifier and present directions for future studies.

2. PM EXPERIMENTAL SETUP

The optical design of our hybrid PM HDFA/TDFA is shown in Fig. 1. A single-frequency input signal at 2051 nm ($\Delta\nu < 2$ MHz) is coupled into a preamplifier consisting of two stages: F1 (3.0 m) and F2 (2.0 m) of PM Ho-doped fiber, iXblue IXF-HDF-PM-8-125. Output from a multiwatt fiber laser P1 at 1941 nm is split by coupler C1 (30%/70%) and is sent to both F1 and F2 via the WDMs. Complete evaluation of the Ho-doped preamplifier is discussed in [8,9]. The preamplifier output provides the signal input to power amplifier F3, a 5.0 m length of double-clad PM Tm-doped fiber (Coherent-Nufern PM-TDF-10P/130-HE). Two multimode multiwatt 793 nm laser sources are coupled into F3 by means of the 2×1 pump combiner PC1. The total pump power at 1941 nm coupled into F1 and F2 is designated P_{p1} , and the total pump power at 793 nm coupled into F3 is designated P_{p2} . In our measurements, input signal power is designated as P_s and output signal power as P_{out} . PM signal light propagates through the fibers and components in the amplifier on the slow fiber axis. Input and output signal powers, pump powers, and NFs are measured internally.

3. DATA FOR THE HO-DOPED AND TM-DOPED FIBERS AND APPROACH TO SIMULATIONS

Summary data for the iXblue PM Ho-doped single-clad silica fiber in our experiments are given below in Table 1.

Fusion splice losses between this fiber and Coherent/Nufern PM1950 passive PM fiber were 0.1 dB or less. The cutoff wavelength for the fiber is 1650 nm.

Figure 2 shows gain and absorption spectra for the $^5I_7 - ^5I_8$ transition of the Ho-doped fiber, which were derived from

Table 1. PM Ho-Doped Fiber Data

Fiber ID	IXF-HDF-PM-8-125
Core diameter, μm	8
Cladding diameter, μm	125
NA	0.15
Fiber structure	PANDA
Birefringence	3.3×10^{-4}
Background loss, dB/m	0.2
Peak absorption, dB/m	57@1951 nm
Ion pairing coefficient, %	10 (Refs. [13–15])
$^5I_7 - ^5I_8$ nonradiative lifetime, mS	0.60 (Ref. [14])

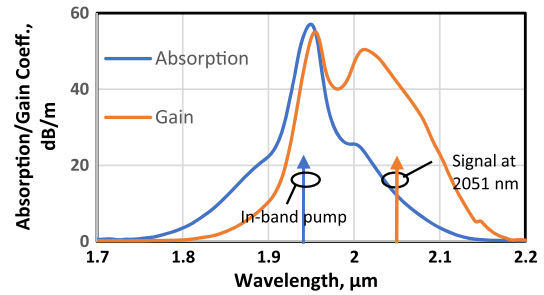


Fig. 2. Gain and absorption spectra for the $^5I_7 - ^5I_8$ transition of the Ho-doped fiber.

measurements by iXblue and data from the literature [11]. The spectral region where the fiber exhibits significant gain clearly extends beyond 2150 nm.

Table 2 gives summary data for the double-clad Tm-doped fiber from Coherent/Nufern.

Splice losses for signal propagation between this fiber and Coherent/Nufern passive PM1950 fiber were estimated to be 0.2 dB or less.

Figure 3 shows our measured values for core gain and core absorption coefficients for the $^3F_4 - ^3H_6$ transition of the double-clad Tm-doped fiber. The peak core absorption was measured to be 468 dB/m at 1645 nm. We note that this fiber has significant gain and very little absorption at the signal wavelength of 2051 nm.

Simulations of single-clad Ho-doped fiber performance used the gain and absorption spectra in Fig. 2 and the data from Table 1 in a two-level Giles model [12] with a saturation parameter of $2.13 \times 10^{18} \text{ m}^{-1} \text{ s}^{-1}$. The ion pairing coefficient accounts for loss of excited state ions caused by detrimental pairwise interactions [13–15]. In our experiments, we chose in-band pumping with $\lambda_p = 1941$ nm, close to the peak of the absorption, as illustrated by the vertical blue arrow in Fig. 2.

The fiber lengths $L_1 = 3.0$ m (first stage) and $L_2 = 2.0$ m (second stage) in the Ho-doped preamplifier were chosen by optimizing the first stage length for maximum simulated gain, and, subsequently, the second stage length for maximum simulated output power, for $\lambda_s = 2051$ nm and an available pump power of $P_{p1} = 4.6$ W at 1941 nm.

Simulation of the double-clad TDFA under 793 nm pumping is represented using a three-level energy model (3H_6 , 3F_4 , and 3H_4) of the thulium ion. This simplified model of the

Table 2. Data for the Coherent/Nufern Double-Clad Tm-Doped Fiber

Fiber ID	PM-TDF-10P/130-HE
Core diameter, μm	10 ± 1
Core NA	0.150
Cladding diameter, μm	130 ± 1
Outer cladding NA	0.460
Cladding attenuation, dB/km	≤ 15 @860 nm
Cladding absorption, dB/m	4.70@793 nm
Birefringence	1.5×10^{-4}
$^3F_4 - ^3H_6$ nonradiative lifetime, mS	0.379 (Ref. [6])

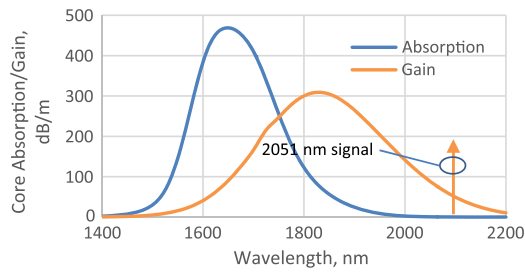


Fig. 3. Core gain and absorption coefficients for the ${}^3F_4 - {}^3H_6$ transition of the Coherent/Nufern DC Tm-doped fiber.

thulium ion is based on a study of the literature; only the relevant transitions were kept. It includes the absorption, gain, and nonradiative transitions between the different levels. Ion-ion interactions are also considered: the well-known 2-for-1 effect and its opposite effect [16]. The steady-state performance simulation is achieved through solving the set of population equations and propagation equations along the active fiber. The accuracy of our simulation software was demonstrated over multiple double-clad amplifier topologies using different active fibers, pumping schemes, and seed wavelength or power [6].

Parameters of the Coherent/Nufern double-clad Tm-doped fiber (given in Table 2 and shown in Fig. 3) were either selected from the literature as representative or measured [17] to simulate this active fiber in our software. The fiber length $L_3 = 5$ m in the Tm-doped power amplifier was chosen by maximizing the simulated hybrid HDFA/TDFA efficiency with the available 793 nm pump power and the optimized output of the preamplifier.

4. EXPERIMENTAL RESULTS FOR THE HYBRID HDFA/TDFA

Figure 4 shows the measured P_{out} as a function of P_{p2} for several values of P_s . The data are plotted in points, and the dotted lines are linear fits to the data. For these data, P_{p1} is held constant at 4.6 W for all values of P_{p2} . The measured values of P_{out} vary linearly with P_{p2} . A maximum optical-optical slope efficiency of $\eta = 54.9\%$ is observed at the maximum input signal power $P_s = +21.1$ dBm. η is defined as the change in output power divided by the change in second-stage pump power, or $\eta = \Delta P_{\text{out}}/\Delta P_{p2}$. The maximum signal output power achieved with this amplifier is 30 W, for $P_{p1} = 4.6$ W at 1941 nm and $P_{p2} = 53.6$ W at 793 nm. The slope efficiency η is greater than the simple quantum limit of 793 nm/2051 nm = 38.7%, clearly indicating the presence of 2-for-1 ion-ion interactions in the double-clad Tm-doped fiber in the power amplifier. We observe from the data that the amplifier reaches saturation at input powers $P_s \approx -10$ dBm by extrapolating from the curves shown in Fig. 4.

Figure 5 plots the measured values of optical-optical slope efficiency η as a function of input power. The points are the data, and the solid line is a polynomial fit to the data. Here $P_{p1} = 4.6$ W at 1941 nm, and $P_{p2} = 53.6$ W at 793 nm. The rapid increase in η as P_s increases is caused by the high gain compression of the three-stage amplifier. For $P_s > -10$ dBm, η is seen to exceed 50%, demonstrating the high

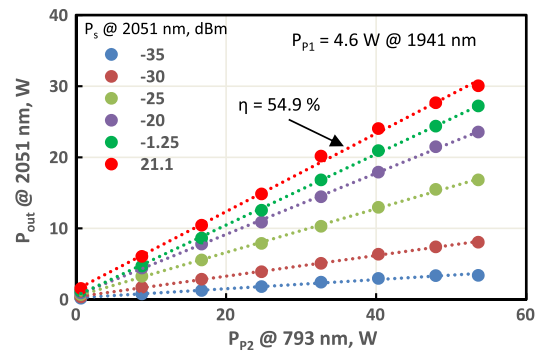


Fig. 4. P_{out} versus second-stage pump power P_{p2} for different signal input powers P_s .

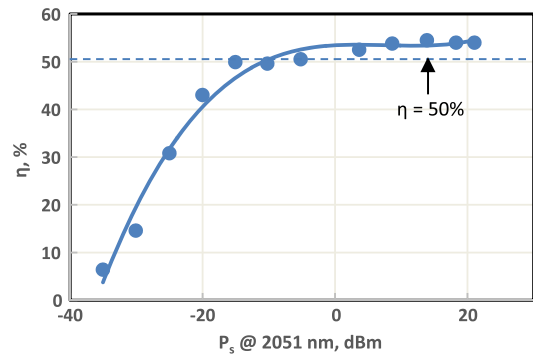


Fig. 5. η versus P_s for $P_{p2} = 53.6$ W.

efficiencies and high dynamic range that can be achieved with the hybrid PM HDFA/TDFA configuration.

Figure 6 shows the measured values of experimental gain G versus input signal power P_s (points) and calculated values of gain (dotted line) for an output power P_{out} of 20 W. For these data, P_{p1} was fixed at 4.6 W at 1941 nm. To achieve $P_{\text{out}} = 20$ W, P_{p2} was adjusted individually for each value of P_s . For $P_s < -26$ dBm, an output power of 20 W could not be achieved; thus, P_{p2} was set to its maximum value of 53.6 W. Here we measure a signal dynamic range for the amplifier of 43 dB for an output power of 20 W.

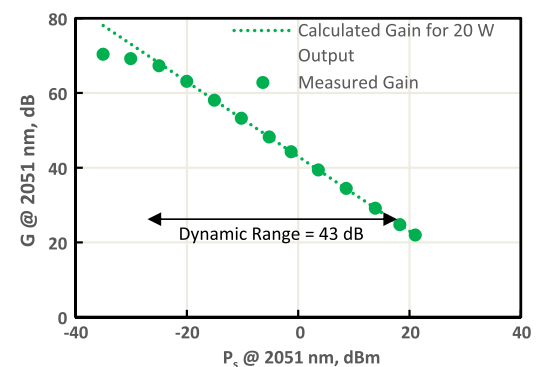


Fig. 6. Measured and calculated gain for 20 W output power.

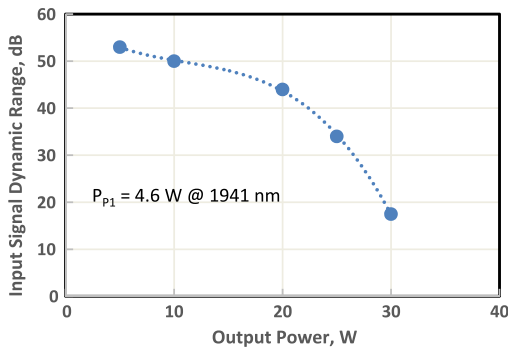


Fig. 7. Input signal dynamic range versus output power.

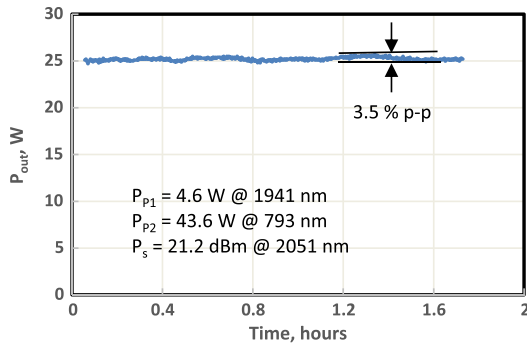


Fig. 8. Long-term stability of output power.

Figure 7 plots the input signal dynamic range as a function of P_{out} . The data are plotted in points, and the dotted line is a polynomial fit to the data. Each point was obtained by measuring the dynamic range at different output powers as described for 20 W P_{out} in Fig. 4. At 25 W output power, the dynamic range has the relatively high value of 34 dB, and this rises monotonically to 52 dB for an output power of 5 W. Such high values of dynamic range are important for successful amplifier operation over wide variations in input signal power.

Figure 8 shows the long-term stability of the amplifier output at an average value of $P_{out} = 25$ W. From these data, we see that the variation in P_{out} over a time period of >1.5 h is 3.5% $p-p$ or 1.25% rms. The data show that the amplifier output is stable for high powers over time and demonstrate good stability.

5. COMPARISON OF SIMULATION AND EXPERIMENT

We begin our comparisons of experiment and simulation by plotting P_{out} as a function of P_s for $P_{p1} = 4.6$ W and four different values of P_{p2} . These data (points) and simulations (solid lines) are shown in Fig. 9, where the simulations are carried out using the techniques detailed in Section 3 for the double-clad TDFA output stage and experimentally measured output powers and output spectra for the single-clad HDFA preamplifier stage. As Fig. 9 demonstrates, agreement between experiment and simulation is good over the measured range of input signal powers and output powers.

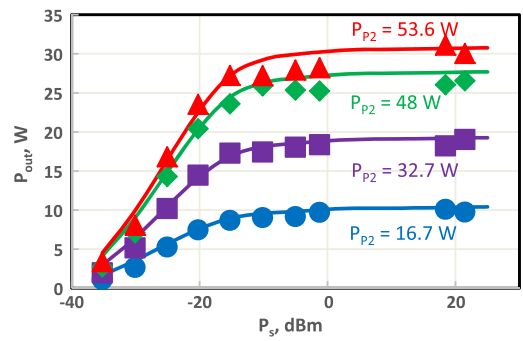


Fig. 9. Experimental (points) and simulated (lines) P_{out} versus P_s for the parameter of P_{p2} .

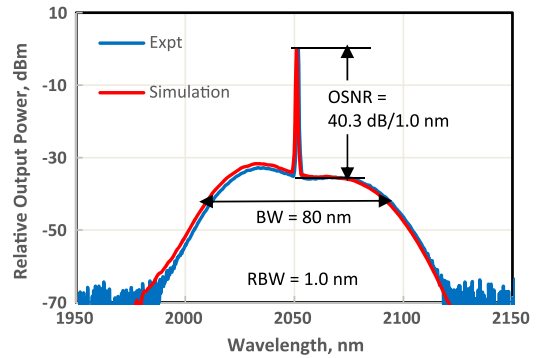


Fig. 10. Experimental and simulated output spectra for $P_s = -5$ dBm.

In Fig. 10, we show the experimental (blue) and simulated (red) output spectra for the three-stage PM HDFA/TDFA for $P_s = -5$ dBm. Here $P_{p1} = 4.6$ W at 1941 nm and $P_{p2} = 53.6$ W at 793 nm. The agreement between data and theory is good, confirming the accuracy of our spectral simulations for this amplifier. We observe that the optical signal-to-noise ratio (OSNR) for this spectrum is 50.3 dB/0.1 nm. An estimate of the amplifier bandwidth made from the -10 dB values of the background amplified spontaneous emission (ASE) spectrum yields $BW = 80$ nm.

Experimental values of in-band OSNR versus P_s , measured just below the peak of the optical signal in Fig. 10, are plotted in Fig. 11. Here we see that the OSNR increases monotonically from 21.2 dB/0.1 nm at $P_s = -35$ dBm to 53.5 dB/0.1 nm at $P_s = -1.3$ dBm. Values of OSNR > 40 dB/0.1 nm are highly desirable for power amplifier applications such as booster amplifiers for coherent lidar systems.

In Fig. 12 we plot G (in blue) and NF (in orange) versus P_s for the indicated values of P_{p1} and P_{p2} . The data are given in points, and the simulations are plotted with solid lines. Our measurements of G and NF are carried out with the optical method as detailed in [18]. The comparison of data and theory shows that the simulations predict the measured G quite well, and that the predicted values of NF are slightly less than the experimental values. For comparison, the values of NF measured for the full three-stage amplifier are quite close to the values measured for the HDFA preamplifier as described

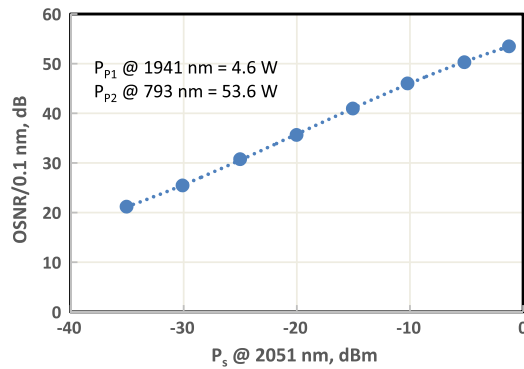


Fig. 11. Measured OSNR as a function of P_s .

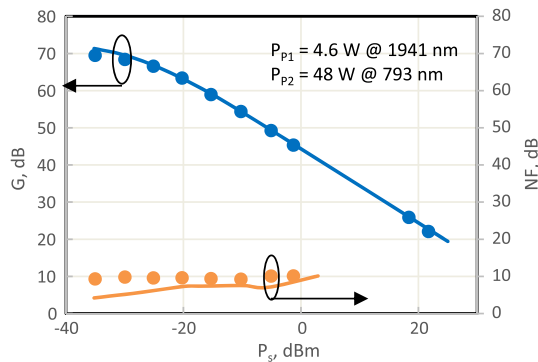


Fig. 12. Experimental and simulated gain and NF versus P_s .

in [8,9]. In reference to the state of the art, Ho-doped amplifier NFs in the small-signal regime of 5–10 dB at 2050 nm have been reported in [19]. We observe that our measured NF is at the upper end of the range given in [19]. The differences between our measured NF values and those reported in [19], and the differences between theory and experiment in Fig. 12, are under active investigation.

Overall, we find that the agreement between simulation and experiment for the three-stage PM HDFA/TDFA is relatively good, indicating that our simulation capabilities accurately represent the physical performance of the multistage optical amplifier.

6. DISCUSSION

The results presented in Sections 4 and 5 indicate that our three-stage PM HDFA/TDFA design is a simple and efficient means to achieve a high slope efficiency of $\eta = 55\%$ (Fig. 4) for the power amplifier configuration with $P_s = +21$ dBm. For high gain applications, the three-stage architecture is quite appropriate, and yields small signal gains of 70 dB. These high gains are important for future applications employing pulsed input sources whose average input power is typically -20 dBm or less. For high input power applications with $P_s > 0$ dBm, the amplifier topology may possibly be simplified to two stages (one Ho-stage preamplifier and one Tm-stage power amplifier) to reduce the cost and complexity of the design.

The high dynamic range of 34 dB at 25 W P_{out} , which rises to 52 dB for $P_{out} = 5$ W, is advantageous in applications using low input powers, e.g., CW preamplifiers and future pulsed source amplification. We believe that the measured NF of 10 dB can be improved by optimizing the design of the Ho-doped fiber in the preamplifier and by optimizing the preamplifier architecture. This topic will be discussed at length in future publications.

The measured NF of the three-stage amplifier is dominated by the NF of the Ho-doped preamplifier, as shown by the theory of discrete concatenated high-gain optical amplifiers [20]. For this reason, the contribution to the total NF from the individual NF of the Tm-doped power amplifier is found to be negligible (<0.2 dB).

The maximum achieved P_{out} of 30 W at 2051 nm is limited only by the power of the 793 nm multimode pump sources in our experiments. We believe that output powers of 50–100 W are readily achievable with higher power pump sources.

From the 10 dB bandwidth of the ASE spectrum underneath the amplified peak signal in Fig. 10, we estimate the effective operating bandwidth of the hybrid PM HDFA/TDFA to be 80 nm. Future work will concentrate on extending this effective operating spectral band to signal wavelengths $\lambda_s > 2100$ nm, a region where there is considerable current interest in atmospheric propagation and directed energy weapons.

Using the parameters for the double-clad Tm-doped fiber in the output power amplifier, with a core diameter of 10 μm and a core NA of 0.15, we expect the M^2 value for the PM HDFA/TDFA to be $M^2 < 1.3$. Future work will directly measure this value to confirm our preliminary estimate.

Future work will also concentrate on direct measurement of the multiwavelength performance of the hybrid amplifier to verify the estimated operating bandwidth of 80 nm.

7. SUMMARY

We have proposed and experimentally demonstrated a new three-stage PM hybrid HDFA/TDFA design exhibiting 30 W output power at 2051 nm. The output power of the existing amplifier is pump-power-limited, indicating that future output powers of 50–100 W should be readily achievable. Our amplifier also exhibits a small signal gain of 70 dB, which is the highest value so far reported for fiber optical amplifiers operating in the 2000 nm region of the spectrum.

A dynamic range of 34 dB at 25 W P_{out} was achieved, rising to 52 dB for $P_{out} = 5$ W. The measured NF of the amplifier is 10 dB over an input power range $P_s = -35$ to -1 dBm. The estimated 10 dB operating bandwidth of the amplifier is 80 nm, and M^2 is estimated to be <1.3 . Measured long term stability at $P_{out} = 25$ W is 3.5% p - p (1.25% rms), illustrating good long-term performance of our amplifier topology.

Comparison of simulations and experiment shows good agreement between theory and data for multiple amplifier operating parameters, validating our approach to calculations of amplifier performance.

Our novel amplifier design points the way toward future applications requiring compact, efficient, high gain, and high-output power fiber amplifiers in the important 2000–2150 nm region of the spectrum.

Acknowledgment. We thank Eblana Photonics, Dublin, Ireland, for single-frequency sources in the 2000 nm band, and iXblue Photonics, Lannion, France, for the PM Ho-doped fiber.

REFERENCES

1. G. D. Spiers, R. T. Menzies, J. Jacob, L. E. Christensen, M. W. Phillips, Y. Choi, and E. V. Browell, "Atmospheric CO₂ measurements with a 2 μm airborne laser absorption spectrometer employing coherent detection," *Appl. Opt.* **50**, 2098–2111 (2011).
2. F. Gibert, A. Dumas, J. Rothman, D. Edouart, C. Cenac, and J. Pellegrino, "Performances of a HgCdTeAPD based direct detection LIDAR at 2 μm: application to DIAL measurements," *EPG Web Conf.* **176**, 01001 (2018).
3. S. Ishii, A. Sato, M. Aoki, K. Akahane, S. Nagano, P. Baron, K. Mizutani, S. Ochiai, and M. Kubota, "Research and development for future space-based Doppler Wind Lidar," in *Proceedings of 18th Coherent Laser Radar Conference* (University of Colorado, 2016), paper M-10.
4. G. D. Goodno, L. D. Book, and J. E. Rothenberg, "Low-phase-noise, single-frequency, single-mode 608 W thulium fiber amplifier," *Opt. Lett.* **34**, 1204–1206 (2009).
5. A. Hemming, N. Simakov, A. Davidson, M. Oermann, L. Corena, D. Stepanov, N. Carmody, J. Haub, R. Swain, and A. Carter, "Development of high power Holmium-doped fibre amplifiers," *Proc. SPIE* **8961**, 89611A (2014).
6. C. Romano, R. E. Tench, and J.-M. Delavaux, "20-W 1952-nm tandem hybrid single and double clad TDFA," *Proc. SPIE* **10512**, 105120Q (2018).
7. R. E. Tench, C. Romano, J.-M. Delavaux, T. Robin, B. Cadier, and A. Laurent, "Broadband high gain polarization-maintaining holmium-doped fiber amplifiers," in *Proceedings of the ECOC*, Rome, Italy, 2018, paper Mo3E.3.
8. R. E. Tench, C. Romano, G. Williams, J.-M. Delavaux, T. Robin, B. Cadier, and A. Laurent, "Two-stage performance of holmium-doped polarization maintaining fiber amplifiers," *IEEE J. Lightwave Technology* **37**, 1434–1439 (2019).
9. R. E. Tench, C. Romano, and J.-M. Delavaux, "Shared pump two-stage polarization-maintaining holmium-doped fiber amplifier," *IEEE Photon. Technol. Lett.* **31**, 357–360 (2019).
10. R. E. Tench, C. Romano, and J.-M. Delavaux, "25 W 2 μm broadband polarization-maintaining hybrid Ho- and Tm-doped fiber amplifier," *Proc. SPIE* **10897**, PW2019 (2019).
11. N. Simakov, A. Hemming, W. A. Clarkson, J. Haub, and A. Carter, "A cladding-pumped, tunable holmium doped fiber laser," *Opt. Express* **21**, 28415–28422 (2013).
12. C. R. Giles, C. A. Burrus, D. DiGiovanni, N. K. Dutta, and G. Raybon, "Characterization of erbium-doped fibers and application to modeling 980-nm and 1480-nm pumped amplifiers," *IEEE Photon. Technol. Lett.* **3**, 363–365 (1991).
13. A. S. Kurkov, E. M. Sholokhov, A. V. Marakulin, and L. A. Minashina, "Effect of active-ion concentration on holmium fibre laser efficiency," *Quantum Electron.* **40**, 386–388 (2010).
14. N. Simakov, "Development of components and fibres for the power scaling of pulsed holmium-doped fibre sources," Ph.D. thesis (University of Southampton, 2017), Section 2.5.
15. J. Wang, D. I. Yeom, N. Simakov, A. Hemming, A. Carter, S. B. Lee, and K. Lee, "Numerical modeling of in-band pumped Ho-doped silica fiber lasers," *J. Lightwave Technol.* **36**, 5863–5880 (2018).
16. G. Friith, D. G. Lancaster, and S. D. Jackson, "85 W Tm³⁺-doped silica fibre laser," *Electron. Lett.* **41**, 687–688 (2005).
17. C. Romano, R. E. Tench, and J.-M. Delavaux, "Simulation of 2 μm single clad thulium-doped silica fiber amplifiers by characterization of the ³F₄–³H₆ transition," *Opt. Express* **26**, 26080–26092 (2018).
18. R. E. Tench, C. Romano, and J.-M. Delavaux, "Optimized design and performance of a shared pump single clad 2 μm TDFA," *Opt. Fiber Technol.* **42**, 18–23 (2018).
19. N. Simakov, Z. Li, Y. Jung, J. M. O. Daniel, P. Barua, P. C. Shardlow, S. Liang, J. K. Sahu, A. Hemming, W. A. Clarkson, S.-U. Alam, and D. J. Richardson, "High gain holmium-doped fibre amplifiers," *Opt. Express* **24**, 13946–13956 (2016).
20. E. Desurvire, *Erbium-Doped Fiber Amplifiers: Principles and Applications* (Wiley, 1994).